VI International Conference on Adaptive Modeling and Simulation
ADMOS 2013
J. P. Moitinho de Almeida, P. Díez, C. Tiago and N. Parés (Eds)

MOVING NODES ADAPTION COMBINED TO MESHLESS METHODS FOR SOLVING CFD OPTIMIZATION PROBLEMS

HONG WANG*, JACQUES PÉRIAUX*† AND ZHI-LI TANG††

*University of Jyväskylä
P.O. Box 35 FI-40014, Jyväskylä, Finland
e-mail: hong.m.wang@jyu.fi

†International Center for Numerical Methods in Engineering (CIMNE)
Edificio C1, Gran Capitán s/n, 08034 Barcelona, Spain
e-mail: jperiaux@gmail.com

††Nanjing University of Aeronautics and Astronautics
Nanjing, 210016, China
e-mail: tangzhili@nuaa.edu.cn

Key words: Adaptive meshless method, Sub-clouds, Nash algorithms, Drag minimization, Multi-objective problem

Abstract. In past decades, many adaptive mesh schemes have been developed and become important tools for designers to simultaneously increase accuracy of their computations and reduce the cost of numerical computations in many engineering problems. In most of the cases the adaptation is done by subdividing cells or elements into finer cells or elements. Maintaining mesh quality during optimization procedure is still a critical constraint to satisfy for accurate design. In the discretized approach using meshless methods, there are no cells or elements but only a cloud of points which flexibility is an advantage compared to the mesh topology constraint. This attractive property facilitates the coupling of meshless methods with adaptive techniques for inverse or optimization problems.

In this paper, an algebraic adaptive meshless scheme based on a weighted reference radius equi distribution is presented. Cloud nodes adaption combined to meshless methods are used to solve inverse and drag minimization Computational Fluid Dynamics (CFD) problems.

The adaptive meshless method coupled with advanced Evolutionary Algorithms (EAs) is considered as a first test case to rebuild via prescribed surface pressure target the shape of the circular arc bump or ogive operating at supersonic shocked flow regimes. The objective functions could be chosen as the distance between candidate and prescribed

pressure coefficients minimized in L_2 norm and uniform level of errors minimized in L_2 norm.

Numerical results demonstrate numerically that adaptive meshless methodology presented in this paper can provide efficiently optimization solutions with a desired accuracy in aerodynamics. Results will be compared with other adaption methods, namely the so called goal oriented method.

1 METHODOLOGY

Based on the success of developing an efficient dynamic cloud technique which maintains the primary clouds of points qualities with rigid moving boundary problems, it is expected to obtain reliable results maintaining the same number of points in the computational domain at each time step or at each modified body shape or position in a design optimization procedure. It is therefore very important to bring an adaptive meshless method to adjust clouds of points automatically.

In past decades, many adaptive mesh schemes have been developed and become important tools for designers to increase the reliability and reduce the cost of numerical computations in many engineering problems. Through an effective adaptive scheme, the discretization error can be reduced via an automatic refinement of the computational region where the accuracy of the numerical solution is low, and therefore the prescribed accuracy [1, 2, 3] is achieved. Hsu et al. [4] proposed an algebraic mesh adaptation scheme based on the concept of arc equidistribution.

1.1 An adaptive meshless method

In this research, an algebraic adaptive meshless scheme based on a weighted reference radius equidistribution is presented. To illustrate this, the difference in 2D Cartesian coordinate system between center point i and its satellite point k can be written as:

$$\begin{cases} \Delta x_{ij} = x_j - x_i \\ \Delta y_{ij} = y_j - y_i \end{cases} \tag{1}$$

For each satellite point j, the distance between center point i and point j is

$$R_{ij} = \sqrt{\Delta x_{ij}^2 + \Delta y_{ij}^2} \tag{2}$$

and the reference radius of cloud C_i is defined as the longest distance between the point i and its satellite point j as

$$R_i = max(R_{i1}, R_{i2}, ..., R_{iM_i}) \tag{3}$$

where M_i is the total number of satellite points around point i. By using the concept of a weighted reference radius equidistribution for mesh from Hsu et al. [4], a weighted reference radius equidistribution for clouds of points based on the pressure gradient in the flow field can be expressed as:

$$\tilde{R}_i = \frac{1}{1 + \beta \mid \nabla P \mid_i} R_i \qquad (4)$$

where β is a constant that controls the sensitivity to the pressure gradient. Thus, the movement of point j should be:

$$\begin{cases} \Delta x'_j = \left(\frac{1}{1+\beta|\nabla P|_i} - 1 \right) \Delta x_j + \Delta x_i \\ \Delta y'_j = \left(\frac{1}{1+\beta|\nabla P|_i} - 1 \right) \Delta y_j + \Delta y_i \end{cases} \qquad (5)$$

considering the movement in point $i(\Delta x_i, \Delta y_i)$.

The adaptive meshless method with a moving technique is implemented and tested on a circular arc bump geometry. The geometry of the channel is depicted in Figure 1 and discretized with 2940 clouds of points distributed in the computational domain. Supersonic flow conditions are Mach number 1.6 and angle of attack 0.0°. These flow conditions are high enough to form a normal shock slightly in front of the bump. This shock bends into an oblique shock, which eventually becomes the foremost oblique shock in a lambda shock structure near the upper wall of the channel. The normal shock segment of the lambda shock has a region of subsonic flow behind it, and the rear-most oblique part of the lambda shock downward intersects the lower wall near the trailing edge of the bump. The pressure contours are shown in Figure 2.

After three rounds of moved points adaptation based on the gradient of pressure in the flow field, Figure 3 presents the moved clouds of points distribution in the computational domain. A higher resolution of the shock can be observed in Figure 4. This comparison demonstrates the advantages of the adaptive meshless method.

1.2 Application to shape reconstruction problems

Since the adaptive meshless method achieves higher solution without adding any points in the flow field, one shape reconstruction test case with the above circular arc bump

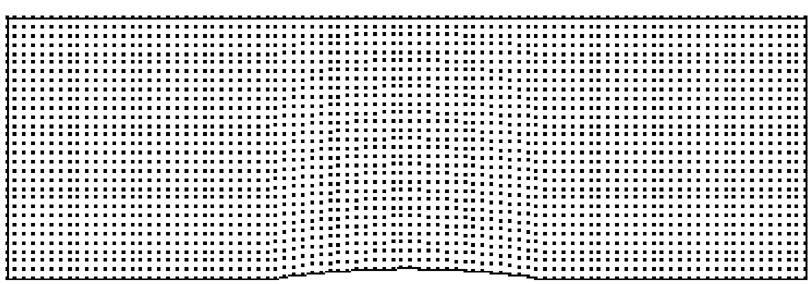

Figure 1: Original clouds of points for the channel with a circular arc bump.

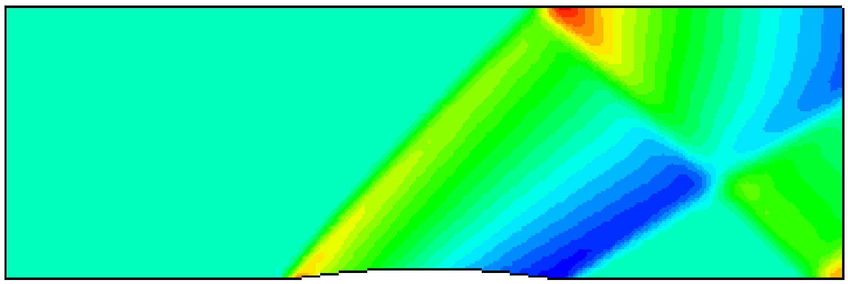

Figure 2: Original pressure contours for the channel with a circular arc bump.

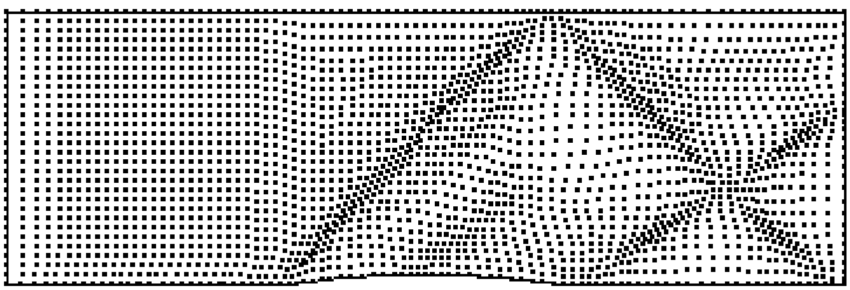

Figure 3: Adapted clouds of points for the channel with a circular arc bump.

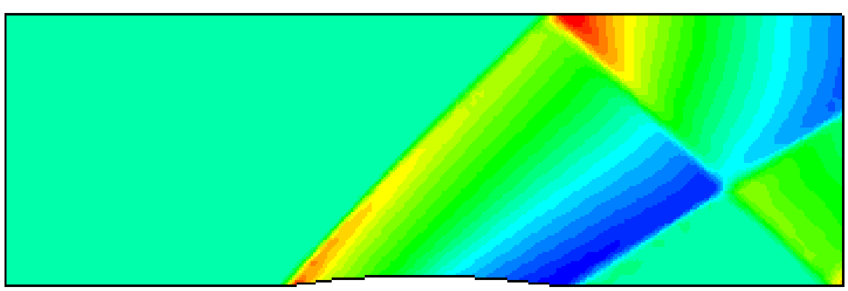

Figure 4: Adapted pressure contours for the channel with circular arc bump.

using adaptive clouds of points is considered in this study. The flow conditions and computational points are the same as in Section 1.1.

Let the thickness of the circular arc bump h be selected as one design parameter. The objective function is defined according to surface pressure coefficients as:

$$\min f(h) = \sum_{i=1}^{M} |C_p(h) - C_p(h^*)|_i^2 \tag{6}$$

where M is the total number of points distributed on the surface of the upper and the lower channel. The search space for the reconstruction is the interval $h \in [2.0, 8.0]$, and h^* is the targeted design parameter. The parameters value in the GA software are the following: 30 the size of population, 0.85 for the probability of crossover and 0.01 for the probability of mutation. The stopping criteria are the fitness value $f(h) < 10^{-06}$ and the number of generation as 50.

Figure 5 shows the convergence history of the objective function reconstruction procedure. Convergence to zero of the fitness function means that GAs coupled with cloud movement have, within 40 generations, successfully rebuilt the circular arc bump with the targeted thickness. Figure 6 is the comparison of surface pressure coefficients of the targeted value and the obtained result. The red solid line stands for the targeted pressure distribution of 5% bump, and blue dots present the obtained pressure distribution of 5.01% bump. The obtained result is in good agreement with the targeted pressure distribution.

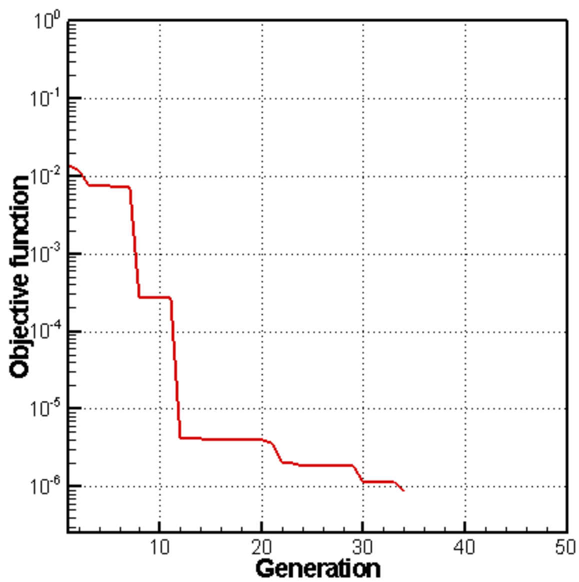

Figure 5: Convergence history of the objective function.

2 CONCLUSIONS

To conclude, the adaptive meshless method coupled with GAs has rebuilt the shape of the targeted circular arc bump based on the prescribed surface pressure. The results presented in this chapter are preliminary and will be consolidated by a measure of the uniformity of level of errors in the flow field to be minimized using sub-clouds and Nash algorithms as a multi-objective problems. The objective functions could be chosen as

f_1, the distance between candidate and prescribed pressure coefficients minimized in L_2 norm, and f_2, uniform level of errors minimized in L_2 norm. Furthermore, distributed optimization coupled with distributed levels of errors can both be run on High Performance Computing (HPC) in the future.

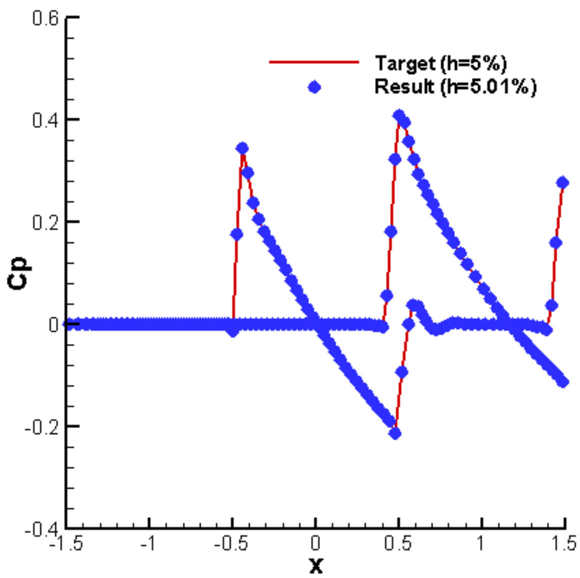

Figure 6: Comparison of pressure distribution of the targeted value and the obtained result.

REFERENCES

[1] Z. Q. Zhu, P. Wang, and X. B. Lu. Adaptive muhigrid solution of the 2D–Euler equations on an unstructured grid. *Acta Mechanica*, 144:43–56, 2000.

[2] A. Anguloa, L. Pérez Pozob, and F. Perazzo. A posteriori error estimator and an adaptive technique in meshless finite points method. *Engineering Analysis with Boundary Elements*, 33(11):1322–1338, 2009.

[3] F. Perazzoa, R. Löhnerb, and L. Perez-Pozo. Adaptive methodology for meshless finite point method. *Advances in Engineering Software*, 39(3):156–166, 2008.

[4] A. T. Hsu and J. K. Lytle. A simple algebraic grid adaptation scheme with applications to two– and three–dimensional flow problems. *AIAA Paper*, 1984, 1989.